



Original Research Paper

Metabolic engineering of the non-conventional yeast *Kluyveromyces marxianus* for enhancing the biosynthesis of succinic acid

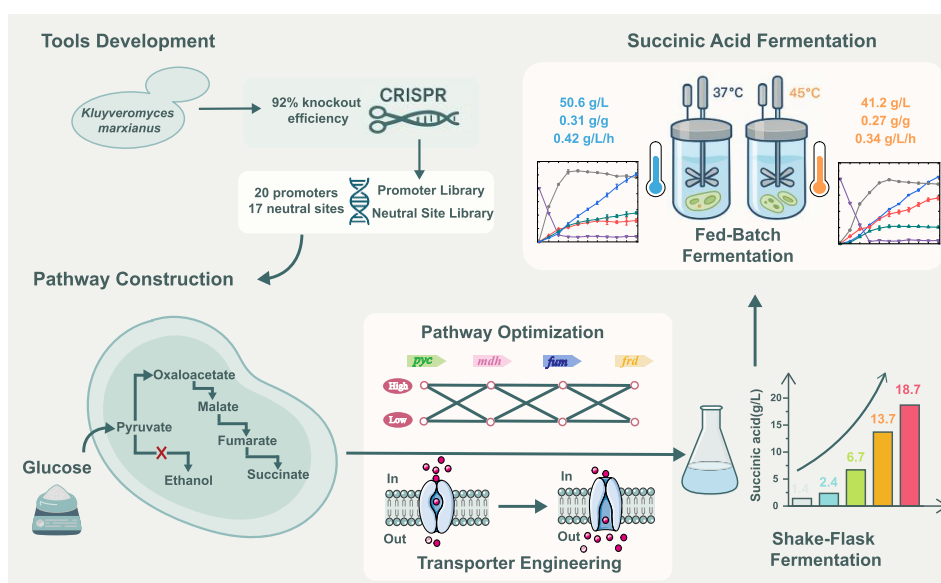
Ziyun Gu, Deyang Ding, Zhanpeng Shan, Yongsheng Tang, Xiulai Chen*

School of Biotechnology and Key Laboratory of Industrial Biotechnology of Ministry of Education, Jiangnan University, Wuxi 214122, China.

HIGHLIGHTS

- The CRISPR-Cas9 system was developed with 92% knockout efficiency in *K. marxianus*.
- 20 promoter and 20 neutral integration sites were identified for stable gene expression.
- The rTCA pathway and transport system were optimized to enhance succinic acid production.
- Succinic acid production with *K. marxianus* KmSA12 was up to 50.6 g/L at 37°C.
- Succinic acid production reached 41.2 g/L at 45°C with a limited amount of neutralizing agents.

GRAPHICAL ABSTRACT



ARTICLE INFO

Article history:

Received 3 April 2025
 Received in revised form 5 June 2025
 Accepted 5 June 2025
 Published 1 September 2025

Keywords:

Kluyveromyces marxianus
 Succinic acid
 Metabolic engineering
 Genetic manipulation
 Thermophilic yeast
 Acid-tolerant fermentation

ABSTRACT

Succinic acid is a crucial four-carbon dicarboxylic acid with widespread applications in the detergent, food, and pharmaceutical industries. However, its microbial production on a large scale is limited by the utilization of neutralizing agents and high cooling costs. In this study, we conducted metabolic engineering of the thermotolerant and acid-tolerant yeast *Kluyveromyces marxianus* to facilitate the efficient biosynthesis of succinic acid at high temperature and low pH. A robust genetic manipulation platform for *K. marxianus* was established by developing gene editing tools, characterizing neutral integration sites, and identifying endogenous promoters. Leveraging this efficient platform, we systematically constructed and optimized the biosynthetic pathway of succinic acid through many metabolic engineering strategies, such as the knockout of byproduct pathways, the redistribution of carbon flux, and the enhancement of the succinic acid transport system. Finally, the engineered strain *K. marxianus* KmSA12 was able to produce 50.6 g/L succinic acid with a yield of 0.31 g/g and productivity of 0.42 g/L/h in a 5-L bioreactor. These results demonstrate the potential of *K. marxianus* as a promising platform for the large-scale production of various organic acids.

©2025 Alpha Creation Enterprise CC BY 4.0

* Corresponding author at:
 E-mail address: xlchen@jiangnan.edu.cn

Contents

1. Introduction.....	2504
2. Materials and Methods.....	2505
2.1. Materials.....	2505
2.1.1. Strains, plasmids, and primers.....	2505
2.1.2. Medium and reagents.....	2505
2.2. Methods.....	2505
2.2.1. Construction of recombinant plasmids and strains.....	2505
2.2.2. Fermentation conditions.....	2505
2.3. Analytical methods.....	2505
2.3.1. Organic acid determination.....	2505
2.3.2. Fluorescence detection.....	2506
2.3.3. Enzyme activity assay.....	2506
2.3.4. qRT-PCR.....	2506
2.3.5. Reactive oxygen species accumulation assay.....	2506
2.3.6. Cell viability assay.....	2506
2.3.7. Membrane integrity assay.....	2506
2.3.8. Protein context assay.....	2506
2.3.9. Metabolic activity assay.....	2506
3. Results and Discussion.....	2506
3.1. Developing genetic manipulation tools in <i>K. marxianus</i>	2506
3.2. Evaluating endogenous promoters.....	2506
3.3. Identifying and screening neutral sites in the genome.....	2508
3.4. Constructing the biosynthetic pathway of succinic acid.....	2510
3.5. Deleting the biosynthetic pathway of byproducts.....	2511
3.6. Optimizing the biosynthetic pathway of succinic acid.....	2511
3.7. Fed-batch fermentation for succinic acid production.....	2511
4. Conclusions.....	2514
Acknowledgements.....	2514
Author contribution.....	2514
Conflict of interest.....	2514
References.....	2514

1. Introduction

Succinic acid is a key platform chemical, identified by the U.S. Department of Energy as one of the twelve most valuable platform compounds (Werpy et al., 2004; Bozell and Petersen, 2010). It has extensive applications in the production of detergents, surfactants, food additives, antimicrobial agents, and pharmaceuticals (Cok et al., 2014). Furthermore, succinic acid serves as a precursor for high-value chemicals such as 1,4-butanediol and tetrahydrofuran, and as a monomer in the synthesis of biodegradable plastics such as polybutylene succinate (PBS) (Choi et al., 2015; Ahn et al., 2016). Driven by increasing demand, the global market for succinic acid is projected to reach USD 205.6 million by 2026, with a compound annual growth rate (CAGR) of approximately 7% (Lee et al., 2019).

Succinic acid is primarily produced through chemical synthesis and biotechnological fermentation. The chemical synthesis involves the hydrogenation of maleic anhydride, derived from C4 fractions in petroleum refining (Jansen and van Gulik, 2014). While this method is well-established and cost-effective, it depends on non-renewable petrochemical resources. Additionally, chemical synthesis requires extreme conditions such as elevated temperatures and pressures, resulting in high energy consumption, environmental pollution, and complex by-products (Liu et al., 2022a). In contrast, microbial fermentation is gaining attention as a more sustainable and environmentally benign alternative. This approach produces succinic acid from renewable biomass, thereby decreasing reliance on fossil resources and promoting green chemistry and sustainable development (Jiang et al., 2017).

Currently, microbial platforms utilized for the biosynthesis of succinic acid primarily consist of bacterial and yeast systems (Table 1). Among bacterial systems, notable examples include *Actinobacillus succinogenes* (Yang et al., 2020), *Mannheimia succiniciproducens* (Lee et al., 2016), *Corynebacterium glutamicum* (Chung et al., 2017; Li et al., 2023), and *Escherichia coli* (Zhu et al., 2014). Recent advancements in genetic engineering have facilitated the construction of several industrial bacterial strains with enhanced capability for succinic acid production. For instance, *C. glutamicum* was modified by introducing a phosphoenolpyruvate

carboxylase (PPC) gene under a strong promoter and deleting the phosphotransferase system (PTS), resulting in a strain capable of producing 152.2 g/L of succinic acid under oxygen-limited conditions (Chung et al., 2017).

While these bacterial hosts can efficiently produce succinic acid, they exhibit several drawbacks, such as obligate anaerobiosis, potential pathogenicity, and low acid tolerance (Zhong et al., 2024). Bacterial fermentation requires continuous addition of neutralizing agents to maintain pH, leading to significant sulfuric acid use for acidification during purification. This requirement not only increases downstream processing costs but also heightens contamination risks during fermentation (Kumar et al., 2020; Oreoluwa Jokodola et al., 2022). In contrast, eukaryotic microorganisms such as *Issatchenkia orientalis* and *Yarrowia lipolytica* exhibit superior acid tolerance and are increasingly investigated for succinic acid production (Yadav et al., 2012). For example, researchers employed various metabolic engineering strategies, including the reexpression of critical pathway enzymes, augmentation of cofactor availability, and optimization of substrate utilization in *I. orientalis* (Tran et al., 2023). The final titer of succinic acid reached 109.5 g/L with a yield of 0.59 g/g, setting a new benchmark for succinic acid production via the reductive tricarboxylic acid (TCA) pathway in engineered yeast. In another study, the reductive TCA (rTCA) pathway was localized to the mitochondria in *Y. lipolytica*, and coupled with adaptive evolution, successfully balanced carbon flux in the oxidative and reductive TCA cycles (Cui et al., 2023). This approach achieved a succinic acid titer of up to 111.9 g/L with a yield of 0.79 g/g glucose in pilot-scale fermentation, underscoring its potential for industrial-scale applications. Despite these advancements in engineering yeasts for succinic acid production, some challenges, such as high cooling costs and extended fermentation times, still hinder large-scale industrialization. Consequently, further yeast engineering is essential to enhance cell growth, temperature tolerance, and acid resistance, thereby reducing production costs and improving economic feasibility.

In this study, we investigated the potential of the thermotolerant yeast *Kluyveromyces marxianus* as a platform for succinic acid biosynthesis, leveraging its rapid growth, robust thermotolerance, and wide substrate spectrum. We developed a highly efficient platform for the biosynthesis of

Table 1.
Comparison of succinic acid production with different strains.

Strain	Temperature (°C)	pH Condition	Titer (g/L)	Yield (g/g)	Productivity (g/L/h)	Ref.
<i>I. orientalis</i> SD108	30	Acidic	109.5	0.63	0.54	Tran et al. (2023)
<i>Y. lipolytica</i> HiSA2	30	Acidic	111.9	0.79	1.79	Cui et al. (2023)
<i>S. cerevisiae</i> PYC2 _{oe} -mpc3Δ sdh1Δ	30	Neutral	45.5	0.66	0.24	Rendulić et al. (2024)
<i>E. coli</i> FM3	37	Neutral	153.4	1.04	2.13	Pan et al. (2024)
<i>K. marxianus</i> KmSA12	37	Neutral	50.6	0.31	0.42	This Study
	45	Acidic	41.2	0.27	0.34	

organic acids through systematic metabolic engineering of *K. marxianus* NBRC 1777. Initially, we constructed a nutrient-auxotrophic chassis strain and established a comprehensive genetic toolkit, which included a CRISPR-Cas9 system, an endogenous promoter library, and a neutral integration site library, to facilitate precise and tunable gene expression. Subsequently, we introduced a heterologous rTCA pathway to enhance succinic acid accumulation. To further optimize metabolic flux, we systematically eliminated byproduct pathways and overexpressed key enzymes with high catalytic efficiency to enhance succinic acid biosynthesis. Additionally, we optimized the transmembrane transport of succinic acid by expressing an efficient dicarboxylate transporter, markedly improving extracellular product accumulation. Finally, in a 5 L bioreactor, the optimized strain *K. marxianus* KmSA12 achieved succinic acid titer, yield, and productivity up to 50.6 g/L, 0.31 g/g, and 0.42 g/L/h, respectively. Furthermore, we performed succinic acid fermentation at 45°C with a limited amount of neutralizing agents; the production of succinic acid with *K. marxianus* KmSA12 reached 41.2 g/L with a yield of 0.27 g/g glucose. This study not only establishes *K. marxianus* as a promising cell factory for bio-based succinic acid production but also offers a robust framework for metabolic engineering of non-conventional yeasts to produce value-added organic acids.

2. Materials and Methods

2.1. Materials

2.1.1. Strains, plasmids, and primers

In this study, *E. coli* JM109 and *K. marxianus* NBRC1777 were used to construct expression vectors and succinic acid-producing strains, respectively. The engineered *K. marxianus* strains used were listed in **Table S1**, and the recombinant plasmids used were listed in **Table S2**.

2.1.2. Medium and reagents

LB medium (10 g/L tryptone, 5 g/L yeast extract, 10 g/L NaCl) was used for routine cultivation of *E. coli*. YPD medium (10 g/L yeast extract, 20 g/L tryptone, 20 g/L glucose) was used for the cultivation of *K. marxianus*. When required, 50 µg/mL ampicillin and 200 µg/mL geneticin were added, respectively. A yeast synthetic defined premixes-SD base (Coolaber, Beijing, China) and yeast amino acids supplement were used for the screening of auxotrophic transformants of *K. marxianus*.

The restriction enzymes, PrimeSTAR DNA polymerase, Taq DNA polymerase, T4 DNA ligase, QucikCut *Dpn* I, and DNA markers were purchased from Takara (Dalian, China). Plasmid extraction kits, gel extraction kits, product purification kits, geneticin (G418), and ampicillin were purchased from Sangon (Shanghai, China). PCR primers were synthesized by Genewiz (Nanjing, China).

2.2. Methods

2.2.1. Construction of recombinant plasmids and strains

Genes were codon-optimized and synthesized by Talen-bio (Wuxi, China). Plasmids were generated by Gibson assembly and Golden Gate

assembly in *E. coli*. *E. coli* plasmids were extracted and verified by restriction digestion. The CRISPR-Cas9 system was utilized for gene deletion in *K. marxianus*. All single-guide RNAs (sgRNAs) were designed using the online tool Cas-Designer (<http://www.rgenome.net/cas-designer/>). The protospacer-adjacent motif (PAM) was the *Streptococcus pyogenes* Cas9 PAM sequence “NGG”. Only sgRNA sequences with minimal predicted off-target effects were selected. Selected sgRNA sequences were cloned into CRISPR plasmid pCAS9 harboring *S. pyogenes* Cas9 under the control of TEF promoter; sgRNA expression was driven by a *K. marxianus*-optimized tRNA–sgRNA fusion cassette. For gene knockout or integration, donor DNA fragments containing ~1000 bp homology arms flanking the Cas9 cut site were synthesized or PCR-amplified. These donor templates were co-transformed with pCAS9 into *K. marxianus* competent cells using a lithium acetate/polyethylene glycol method (Antunes et al., 2000). Transformants were plated on SC-URA plates and incubated at 37 °C for 48-72 h.

2.2.2. Fermentation conditions

For succinic acid production in shake flasks, *K. marxianus* was initially propagated on agar plates overnight at 37°C. Subsequently, a single colony was selected for seed cultures, which were then cultivated in 30 mL YPD medium for 12 h. Next, seed cultures were inoculated with 10 mL into 100 mL of fermentation medium and cultivated at 37°C and 200 rpm for 8 h. Subsequently, the culture was transferred to a 500 mL shake flask for microaerobic fermentation at 37°C and 100 rpm for 72 h. The glucose concentration was maintained at 0-20 g/L. CaCO₃ was added to regulate the pH at 5.5-6.5.

For succinic acid production in a 5-L bioreactor, the seed culture method was consistent with that used in shake flasks. Subsequently, seed cultures were inoculated into 3 L of fermentation medium at a 10% (v/v) inoculation rate and cultured at 37°C (or 45°C) for 120 h. After 12 h, dissolved oxygen was maintained at approximately 10% by adjusting agitation speed and aeration rate, ensuring proper fermentation during the microaerobic stage for 108 h. When initial glucose (40 g/L) was depleted during fermentation, 800 g/L of glucose was fed to maintain glucose concentration at 0-5 g/L. For 37°C fermentation, CaCO₃ was added to regulate the pH at 6.0-6.5. For 45°C fermentation, 20 g/L CaCO₃ was added at the beginning of fermentation to regulate the pH, and during the following fermentation process, no additional neutralizing agents were used.

2.3. Analytical methods

2.3.1. Organic acid determination

The culture broth was centrifuged at 12000 rpm for 5 min, and supernatants were obtained for analysis of extracellular metabolites and sugars. Glucose, glycerol, ethanol, succinic acid, pyruvic acid, and other byproducts of broths were analyzed and quantified using HPLC with UV and RID detectors (Shimadzu, Kyoto, Japan). Metabolites and sugars were analyzed at 52°C with 5 mM H₂SO₄ as the mobile phase, with a flow rate of 0.6 mL/min.

2.3.2. Fluorescence detection

Seeds were inoculated into YPD medium, cultured at 37°C (or 45°C) overnight, and then adjusted to an optical density at 600 nm (OD₆₀₀) of 0.1 for cultivation. Samples were harvested and analyzed at 36 h, 48 h, and 60 h. 200 µL dilution was used for fluorescence detection by a microplate reader. The eGFP fluorescence intensity was measured with excitation and emission wavelengths of 485 nm and 525 nm, respectively. Culture density was also measured as the absorbance at 600 nm.

2.3.3. Enzyme activity assay

A single colony was picked from plates and inoculated into 50 mL SC-URA medium in 250 mL shake flasks. The culture was incubated at 37°C with shaking at 200 rpm for 16 h. *K. marxianus* cells were harvested, centrifuged, and washed twice with ice-cold PBS (pH 7.4). After that, cell pellets were resuspended in 1 mL PBS. To lyse these cells, 0.6 g acid-washed glass beads were added, and the suspension was vortexed for two cycles, each lasting 10 min (66 Hz, 30 s on, 30 s off, 10 cycles). The cell lysate was centrifuged at 8,000 rpm for 10 min at 4°C to remove cell sediments, and the supernatant was collected for enzyme activity assays. For pyruvate carboxylase (PC) activity, the reaction mixture contained PBS (pH 7.6), 7.5 mmol/L MgSO₄, 0.1 mmol/L acetyl-CoA, 20 mmol/L KHCO₃, 0.1 mmol/L NADH, 10 mmol/L pyruvate, 4 mmol/L ATP, and 1 µL MDH. The enzyme reaction was initiated by adding cell lysate, and the absorbance at 340 nm was monitored. For malate dehydrogenase (MDH) activity, the reaction mixture consisted of PBS (pH 7.4), 1 mmol/L oxaloacetate, 0.1 mmol/L NADH, and cell lysate. The absorbance at 340 nm was recorded. For fumarase activity, the reaction mixture contained Tris-HCl (pH 7.8), 50 mmol/L malate, and cell lysate. The absorbance at 250 nm was measured. Protein concentrations were determined using the modified Bradford assay (Bradford, 1976).

2.3.4. qRT-PCR

Yeast cells were harvested from 24 h fermentation broth and washed twice with PBS by resuspension and centrifugation at 6,000 rpm for 5 min at 4°C. The cell disruption method was obtained by liquid nitrogen freeze grinding. Total RNA was isolated using the EASY spin Yeast RNA Quick Extraction kit (1 µg of total RNA was taken to synthesize cDNA by using a PrimeScript II 1st-Strand cDNA synthesis kit). The cDNA mixture was diluted to about 30 ng/µL and then used as the template for analyzing the gene expression level by quantitative reverse transcription-PCR (qRT-PCR) with SYBR Premix Ex Taq using an iQ5 continuous fluorescence detector system. The *act1* expression level was used for normalization.

2.3.5. Reactive oxygen species accumulation assay

Endogenous levels of reactive oxygen species (ROS) were measured using a fluorometric assay employing 2',7'-dichlorofluorescein diacetate (DCFH-DA). Briefly, *K. marxianus* cells were collected from 24 h fermentation broth in a 5-L bioreactor, then centrifuged, washed, and resuspended to an OD₆₀₀ of 1.0 in 1 mL PBS. DCFH-DA was added to the cell suspension at a final concentration of 10 µM. After incubation, the fluorescence intensity (excitation at 488 nm, emission at 525 nm) was measured using a SpectraMax M3 spectrofluorometer.

2.3.6. Cell viability assay

For the assessment of cell viability, propidium iodide (PI) staining was performed. 1 mL of cell culture was collected, washed twice with PBS, and resuspended to an OD₆₀₀ of 0.4 in 1 mL PBS. Then, 5 µL Propidium Iodide (PI) was added to the cell suspension, which was then incubated for 20 min at 37°C in dark conditions. Cell viability was assessed by flow cytometry.

2.3.7. Membrane integrity assay

In the membrane integrity assay, 1 mL of the cell culture was taken, washed twice with PBS, and resuspended to an OD₆₀₀ of 0.4 in 1 mL PBS. Then, 5 µL SYTOX was added to the cell suspension, and incubated for 5 min at 37°C in dark conditions, and then used for flow cytometry analysis.

2.3.8. Protein context assay

To measure protein contents, 1 mL of the cell culture was collected and washed twice with PBS. Subsequently, the samples were centrifuged at 5000 rpm for 2 min, and the culture medium was discarded. Then, 10 mg yeast sludge was weighed, resuspended in 1 mL PBS, and disrupted with an ultrasonic cell disintegrator for 15 min. The supernatant was collected by centrifugation at 12,000 rpm for 5 min, and then the protein contents were measured by a BCA Protein Assay Kit.

2.3.9. Metabolic activity assay

One mL of cell culture was taken, washed twice with PBS, and resuspended to an OD₆₀₀ of 10 in 1 mL PBS. Resazurin solution (1 g/L) was added to the suspension at a 10 % (v/v) ratio and incubated at 37°C in dark conditions with shaking for 2 h. After incubation, the fluorescence intensity (excitation at 560 nm, emission at 590 nm) was measured using a SpectraMax M3 spectrofluorometer.

3. Results and Discussion

3.1. Developing genetic manipulation tools in *K. marxianus*

To facilitate genetic manipulation of *K. marxianus*, we constructed a nutrient-auxotrophic strain. Initially, the *ura3* gene, encoding orotidine-5'-phosphate decarboxylase, was knocked out by replacing it with a G418 (geneticin) resistance marker via homologous recombination (Fig. 1a). Subsequently, the *leu2* (encoding 3-isopropylmalate dehydrogenase) and *trp1* (encoding phosphoribosylanthranilate isomerase) genes were replaced using HisG-URA3-HisG deletion cassettes to generate additional selection markers (Fig. 1b). Ultimately, *K. marxianus* strain Km003 was successfully developed, which is auxotrophic for uracil, leucine, and tryptophan. Gene deletions were confirmed by genomic PCR, and the auxotrophic phenotypes were validated on SC plates supplemented with the corresponding amino acids (Fig. 1c).

To improve the efficiency of gene knockout, the CRISPR-Cas9 system was developed. The *adel* gene encoding phosphoribosylaminoimidazole synthase was selected as a reporter gene to evaluate the effectiveness of this system. Disruption of the *adel* gene in *K. marxianus* resulted in mutant strains forming red colonies on adenine-deficient media. An sgRNA targeting the *adel* gene was first designed and inserted into the pCAS9 plasmid. Then, the recombination plasmid pCAS9-ADE1 was transformed into strain Km003. On the transformation plate, 468 colonies were observed, of which 110 colonies exhibited the characteristic red color. Although the total colony count was decreased by 26.3% compared to that of the homologous recombination-based *adel* knockout, the knockout efficiency with the CRISPR-Cas9 system was increased by 180%.

To further increase the efficiency of the CRISPR-Cas9 system, the effect of homologous repair templates was investigated by introducing a repair fragment containing 1,000 bp homologous regions flanking the *adel* locus. This repair fragment was co-transformed with the recombination plasmid pCAS9-*adel* into strain Km003, yielding 137 colonies, of which 126 colonies exhibited the red phenotype. The knockout efficiency of the CRISPR-Cas9 system reached 92% (Figs. 1e and f). These results demonstrated that the CRISPR-Cas9 system facilitated precise and efficient gene targeting in *K. marxianus* with high knockout efficiency.

3.2. Evaluating endogenous promoters

Recent investigations have focused on a variety of promoters derived from *S. cerevisiae* for potential applications in *K. marxianus*. Ten endogenous constitutive promoters have been identified, achieving a 40-fold range in gene expression (Rajkumar et al., 2019). However, their performance across different growth phases and environmental conditions has not been thoroughly examined. To facilitate the regulation of differential gene expression in *K. marxianus*, the strength of endogenous promoters was predicted and evaluated. The Basic Local Alignment Search Tool (tBLASTn) was used to select 20 genes associated with glycolysis, the pentose phosphate pathway, the TCA cycle, and primary metabolic

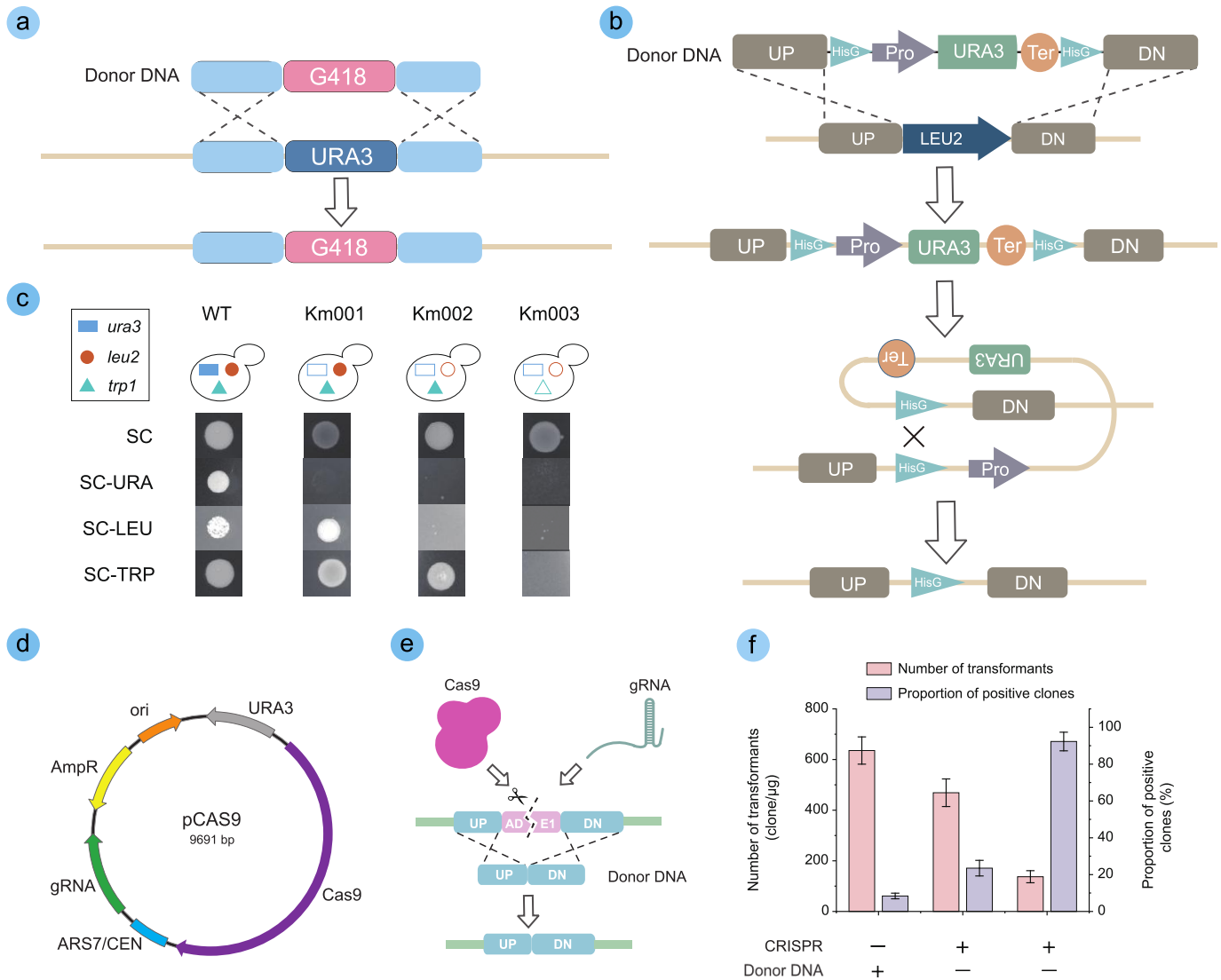


Fig. 1. Developing genetic tools for *K. marxianus*. **a:** Homologous recombination for *ura3* knockout. **b:** Deletion of *leu2* and *trp1*. **c:** Phenotypic verification of the auxotrophic strain Km003. **d:** The schematic map of the pCAS9 plasmid elements. **e:** The *ade1* gene knockout mediated by the CRISPR-Cas9 system. **f:** The knockout efficiency using different gene knockout methods.

pathways. The 1000 bp regions upstream of their start codons were extracted as putative promoter sequences. These genes included TEF1, PDC1, PGK1, GPD1, GPD2, FBA1, HHF1, GDH2, ADH1, and MDH1, among others (Table S3).

To evaluate the relative strength of the identified promoters, an endogenous promoter-eGFP reporter plasmid (pGFP) was constructed. This plasmid was subsequently used to express green fluorescent protein (eGFP) under the control of the respective promoters. Following transformation into Km002, fluorescence intensity was measured for the recombinant strains cultured in SC-LEU medium at 37°C for 60 h (Fig. 2a). Consequently, a promoter library was successfully constructed, and promoter strengths were evaluated at 37°C using glucose as the carbon source.

The ADH1 promoter exhibited the highest expression strength, followed by the PDC1 and ADH2 promoters, which were categorized as strong promoters. Promoters exhibiting strengths below 33.3% of ADH1 were classified as weak promoters, while the remaining promoters were designated as intermediate strength. During the logarithmic phase, the promoters of glycolysis and cell growth-related genes, such as TEF1 and HHT1, exhibited the highest activity. In contrast, during the later

logarithmic and stationary phases, the promoters of genes associated with ethanol production, such as ADH1 and PDC1, showed significantly higher activity, reaching up to 7.25 times compared to that of weak promoters. These results demonstrated the successful development of an endogenous promoter library that enables stage-specific and variable regulation of gene expression across different growth phases.

Temperature control during fermentation is associated with production cost, and thus, *K. marxianus* is often utilized in industrial production under high-temperature fermentation conditions. Under these elevated conditions, the expression levels of the same gene may vary significantly. Promoter strength was further evaluated at 45°C (Fig. 2b), revealing a significant decrease for most promoters at 45°C compared to 37°C. However, HHT1 and PGK1 promoters remained stable and were the most robust promoters at 45°C. The remaining promoters were categorized into seven medium-strength and eight weak-strength promoters based on fluorescence intensity. At 45°C, genes associated with chromosomal repair and protein stability, such as HHT1 and HSP26, exhibited enhanced promoter strength, whereas promoters associated with glycolysis and the TCA cycle showed reduced promoter strength. This observation is likely due to 45°C approaching the

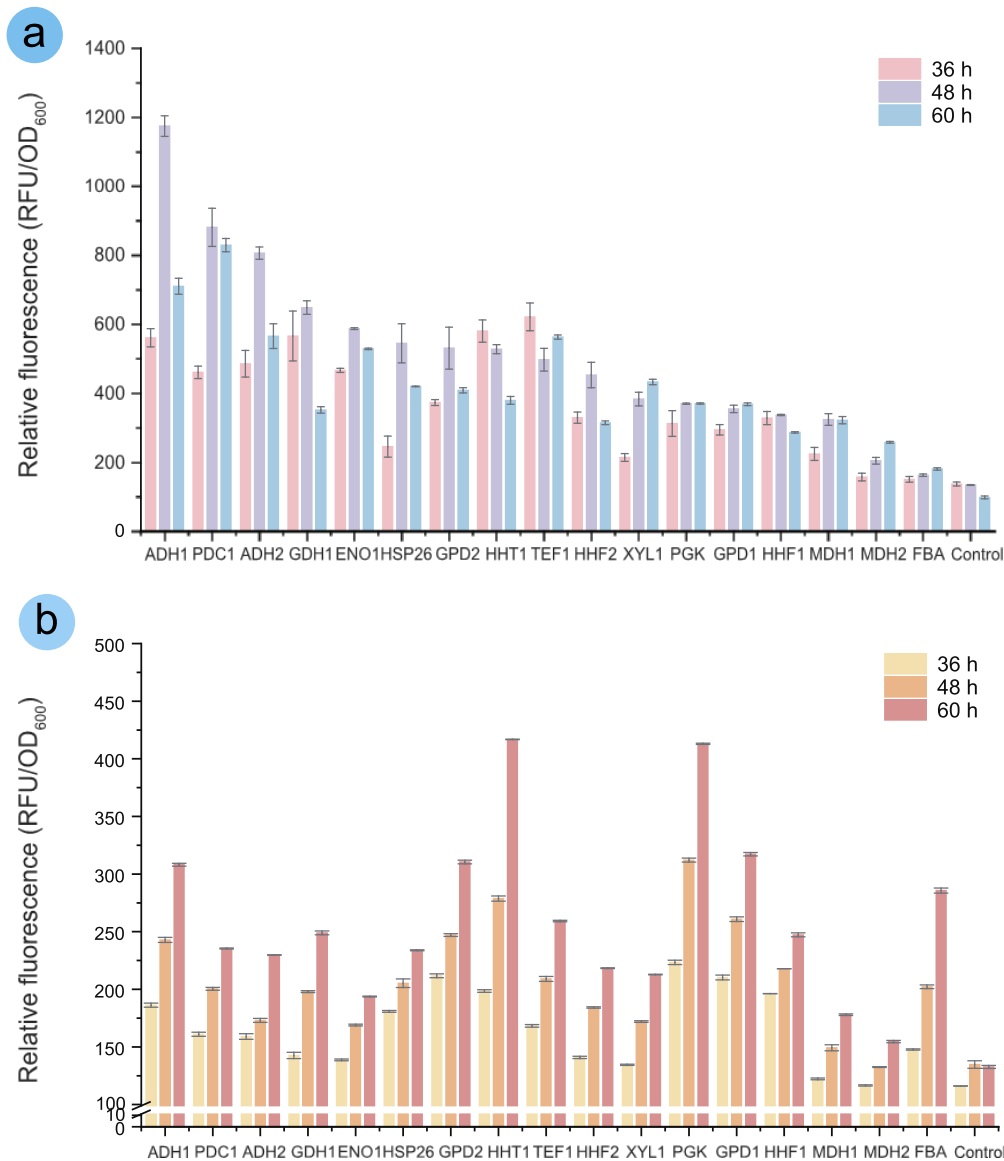


Fig. 2. The expression levels of eGFP driven by different endogenous promoters at various cell growth stages. **a**: promoter strength at 37°C. **b**: promoter strength at 45°C.

heat stress threshold for yeasts, favoring the expression of heat shock proteins and stress-responsive genes, thereby influencing promoter strength (Xiong et al., 2018).

Promoters linked to ethanol biosynthesis exhibit significantly reduced activity at 45°C compared to their robust performance at 37°C, while those involved in glycerol biosynthesis maintain relatively high levels of activity. This difference may be attributed to the metabolic strategy of yeasts, which favors the rapid consumption of carbon sources and the generation of ATP through ethanol fermentation at 37°C. However, at 45°C, the elevated temperature can intensify the toxic effects of ethanol on cellular membranes and proteins, resulting in the downregulation of ethanol synthesis-related genes through promoter regulation (Riles and Fay, 2019). Conversely, glycerol serves as a critical protective metabolite against heat stress.

At 45°C, yeasts may upregulate the expression of glycerol synthesis-related genes through signaling pathways, such as the HOG pathway, to counteract heat stress (Dunayevich et al., 2018). In this context, certain core promoters, specifically TEF1 and HHT1, maintained high activity at 45 °C

despite the overall alterations in promoter dynamics. TEF1 and HHT1 are known as robust and constitutive promoters in yeasts. The TEF1 promoter is particularly used for protein expression due to its sustained activity across various conditions, indicating its inherent thermotolerance. Similarly, HHT1, encoding a histone H3 variant, plays a crucial role in maintaining chromatin integrity and genome stability, which are vital under thermal stress (Takayama and Takahashi, 2007). The sustained activity of these promoters at elevated temperatures likely reflects their critical contributions to the preservation of fundamental cellular processes, including protein synthesis and nucleosome assembly during heat stress.

3.3. Identifying and screening neutral sites in the genome

The biosynthesis of metabolic products often necessitates the overexpression of multiple enzymes involved in metabolic pathways. Plasmid-based expression systems generally require various selection markers, imposing a metabolic burden on cells and increasing the risk of

plasmid loss during fermentation processes. The identification of specific genomic integration sites provides an alternative approach, facilitating the stable and efficient expression of heterologous genes to meet the demands of pathway construction. Furthermore, certain genomic regions may cause gene silencing or overexpression, which could adversely affect cell performance. To mitigate these drawbacks, it is essential to select suitable integration sites for stable gene expression. Therefore, the screening for neutral integration sites in the yeast genome represents a key strategy for enhancing the efficiency of metabolic engineering and the stability of the strain. Recently, several intergenic regions in *K. marxianus* have been identified, and six out of eight regions could facilitate efficient gene integration without compromising cell growth, thereby offering promising avenues for strain engineering in this yeast species (Zhou et al., 2024). Despite these advancements, the limited availability of well-characterized integration sites still hinders the full potential of *K. marxianus* as a robust industrial cell factory.

The *K. marxianus* genome was analyzed to identify potential neutral integration sites for heterologous gene expression based on the following criteria: (i) localization in intergenic regions flanked by two genes with a minimum intergenic distance of 700 bp; (ii) high efficiency of gene integration; (iii) facilitation of elevated heterologous gene expression; and (iv) minimal impact on cell growth. Using online prediction tools CRISPR-COPIES and transcriptomic datasets previously reported for *K. marxianus* (Lertwattanasakul et al., 2015), 20 candidate intergenic regions were

identified. These sites were distributed across eight chromosomes and spaced sufficiently to prevent recombination events that could result in the loss of a genomic fragment (Fig. 3a).

To evaluate integration efficiency at different neutral sites, the CRISPR-Cas9 system was utilized to integrate an eGFP expression cassette into each candidate location (Fig. 3b). Successful integration was achieved at 17 sites, while the remaining sites failed, likely due to their essential roles in cell growth, as the insertion of a heterologous gene resulted in cell lethality. Both bright-field and fluorescence microscopy confirmed eGFP expression in colonies from all successful transformations.

Further analysis of fluorescence intensity and cell growth revealed variations in eGFP signals and growth states among strains with different integration sites, indicating that the location and architecture of gene integration significantly affect gene expression and cellular performance (Figs. 3c and 3d). Among the identified integration sites, NS3, NS6, NS8, NS10, NS11, NS12, and NS19 exhibited strong fluorescence protein expression, rendering them particularly suitable for high-level gene expression. In contrast, NS4, NS5, NS7, NS11, NS13, and NS16 exhibited favorable growth characteristics, suggesting their suitability for gene integration. Considering both fluorescence intensity and growth performance, NS8, NS12, and NS19 were identified as the most optimal candidates for heterologous gene expression. These results highlight the potential of neutral integration sites to effectively regulate gene expression and maintain the balance of metabolic pathways.

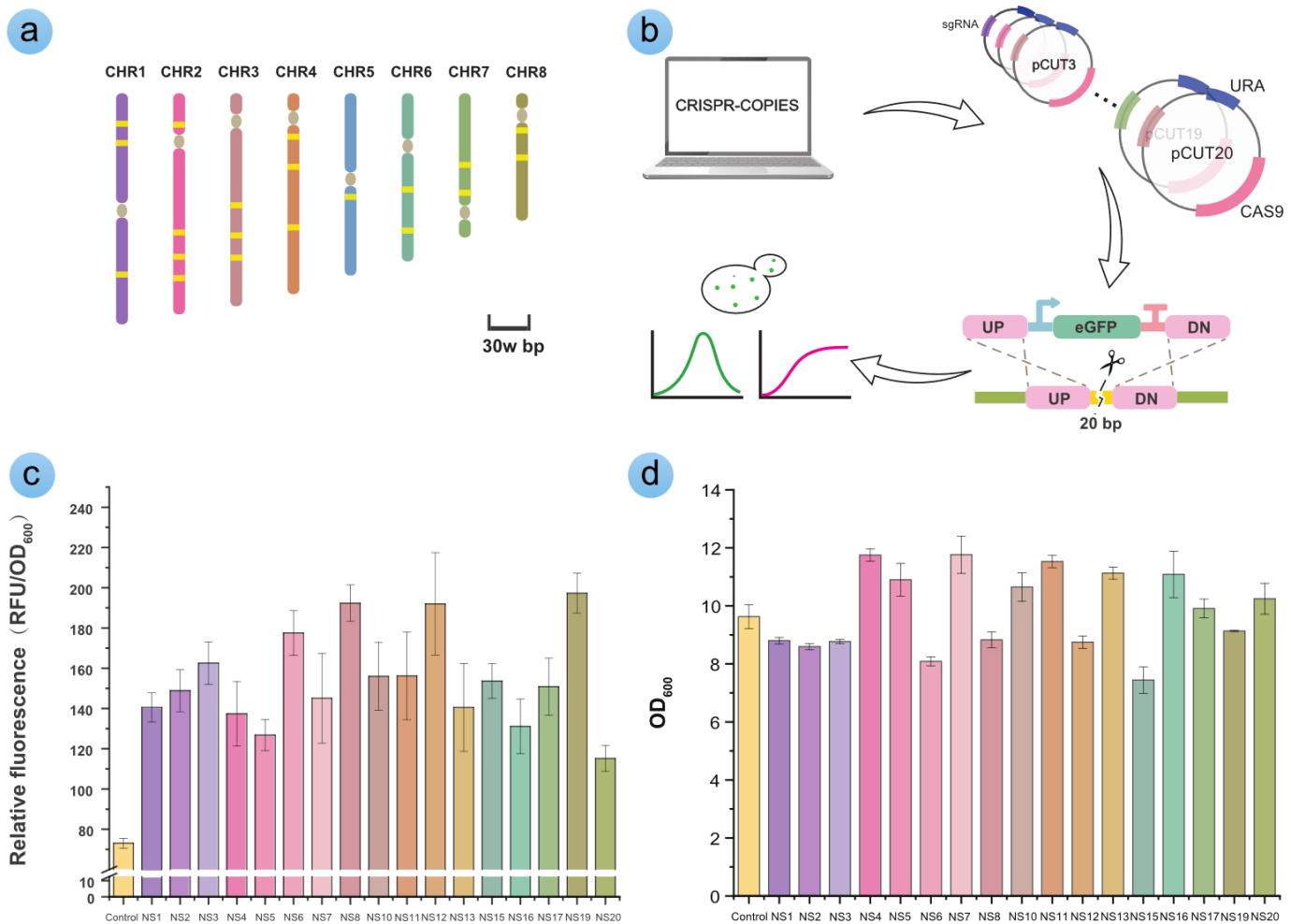


Fig. 3. Identifying and screening neutral sites in the genome. a: Screening and selecting potential neutral integration sites. b: Cas9-based toolkit for eGFP expression in *K. marxianus*. c: The eGFP expression level from different neutral sites. d: The cell growth from different neutral sites.

During the process of screening neutral sites, we observed significant variability in eGFP expression across various neutral sites, leading us to hypothesize that this variability may be influenced by chromatin context and transcriptional interference. Many factors, such as histone modifications, DNA methylation patterns, and proximity to heterochromatin domains, can significantly impact transgene expression levels. When genes were located near heterochromatin regions, they may experience transcriptional silencing or diminished expression due to alterations in chromatin structure (Liu, et al., 2022b).

Transcriptional interference (TI) contributes significantly to expression variability, occurring when transcription at one genomic locus negatively affects neighboring gene expression, especially in convergent gene orientations (Eszterhas et al., 2002). In such cases, convergent transcription units may experience mutual suppression of expression, while divergent ones show minimal interference. This suggests that TI influences eGFP expression at neutral sites near active genes. Additionally, promoter occlusion and epigenetic regulation are also likely contributing factors. The

active transcription of one gene may obscure the promoter of a neighboring gene, hindering the binding of transcription machinery and consequently reducing gene expression.

3.4. Constructing the biosynthetic pathway of succinic acid

The rTCA pathway, the oxidative TCA cycle, and the glyoxylate shunt represent the primary metabolic routes for succinic acid biosynthesis (Fig. 4a). Among these pathways, the rTCA pathway has the highest theoretical yield of 1.31 g/g when glucose is used as the substrate. The conversion of pyruvic acid to succinic acid via the rTCA pathway mainly consists of pyruvate carboxylase (PYC), malate dehydrogenase (MDH), fumarase (FUM), and fumarate reductase (FRD). In the process of succinic acid biosynthesis, MDH and FRD consume two moles of NADH, establishing NADH as a critical limiting cofactor. These findings highlight the significant influence of intracellular NADH availability on the efficiency of the rTCA pathway. Since these enzymes function in a reverse manner or are

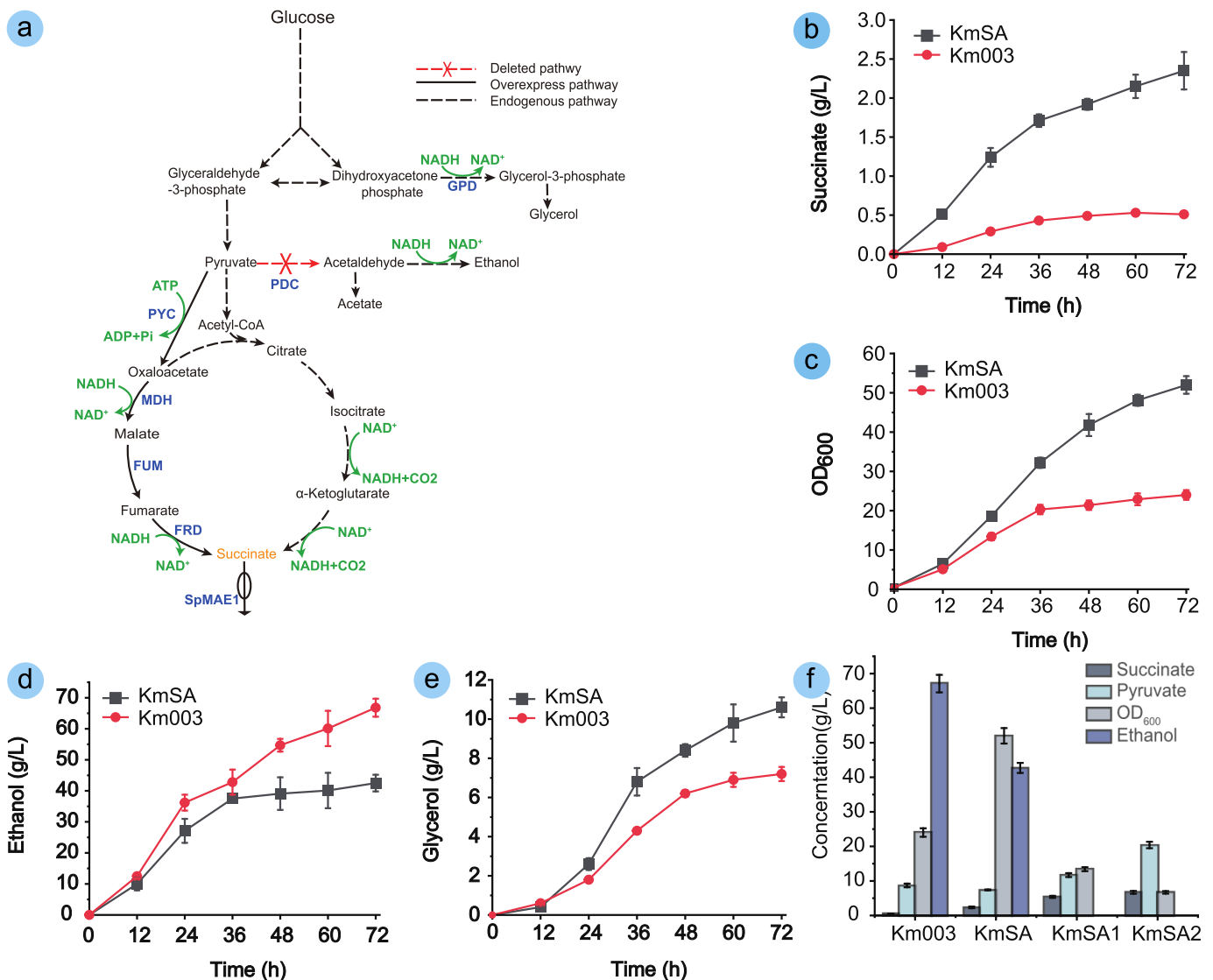


Fig. 4. Constructing the biosynthetic pathway of succinic acid. **a:** The biosynthetic pathway of succinic acid with genetic modification. **b:** Effect of the heterologous rTCA pathway on succinic acid accumulation. **c:** Effect of the heterologous rTCA pathway on cell growth. **d:** Effect of the heterologous rTCA pathway on ethanol accumulation. **e:** Effect of the heterologous rTCA pathway on glycerol accumulation. **f:** Effect of the ethanol and glycerol synthesis pathway on succinic acid, pyruvate, cell growth, and ethanol.

located in different cellular compartments, their heterologous expression was introduced into *K. marxianus* to establish a functional rTCA pathway for succinic acid production.

To construct the heterologous pathway for succinic acid biosynthesis, we selected the pathway enzymes from diverse sources, guided by an extensive literature review and database analysis. The *PYC* gene was obtained from *Aspergillus flavus*, a fungus well known for its high L-malate production. The *MDH* gene was isolated from *Actinobacillus succinogenes*, a natural succinic acid producer. The *FUM* gene (*fumC*) from *E. coli* was expressed to catalyze the conversion of malate to fumarate in the cytosol. The final enzymatic step, which involves the conversion of fumarate to succinate, was catalyzed by the cytosolic *FRD* from *Trypanosoma brucei*, known for its efficiency in enhancing succinate production with NADH as a cofactor. All genes were codon-optimized, and signal peptides were removed to ensure the localization of proteins in the cytosol.

To enhance succinic acid production in *K. marxianus*, the biosynthetic pathway was optimized by enhancing the rTCA pathway. The genes *Appyc*, *Asmdh*, *EcfumC*, and *Tbfrd* were expressed under the robust promoters *P_{PDC1}* and *P_{ADHI}* in *K. marxianus*. These expression cassettes were integrated into the genome of strain Km003 (NBRC1777 Δ *ura3* Δ *leu2* Δ *trp1*). Following the simultaneous overexpression of these genes, the engineered strain KmSA produced 2.35 g/L succinic acid, representing a 67.8% increase compared to that of Km003 (Fig. 4b). Additionally, the maximum OD₆₀₀ reached 52, representing a 116% improvement over Km003 (Fig. 4c). These findings indicated that the construction of the rTCA pathway in *K. marxianus* successfully enhanced succinic acid accumulation without negatively affecting cellular metabolism or cell growth. Nonetheless, succinic acid production remains limited, underscoring the necessity for additional metabolic engineering efforts to enhance the production of succinic acid.

3.5. Deleting the biosynthetic pathway of byproducts

During fermentation for succinic acid production with strain KmSA, ethanol was identified as the primary byproduct, reaching 32.5 g/L (Fig. 4d). Ethanol is produced through the reduction of acetaldehyde, catalyzed by NADH-dependent alcohol dehydrogenase (*ADHI*) (Geng et al., 2024). As the rTCA pathway for succinic acid production also requires NADH, the competition for precursor metabolites and cofactors between ethanol accumulation and succinic acid production likely limits the efficiency of succinic acid biosynthesis (Wang et al., 2023). To alleviate this competitive interaction, we knocked out *PDC1* (encoding pyruvate decarboxylase), resulting in strain KmSA1. This modification eliminated ethanol accumulation in strain KmSA1, but resulted in a 37.1% reduction in OD₆₀₀. During shake flask fermentation, strain KmSA1 accumulated 6.7 g/L succinic acid, representing a 185.1% increase compared to that of strain KmSA. Notably, pyruvate accumulation was increased to 20.6 g/L, replacing ethanol as the main byproduct.

The deletion of key genes involved in glycerol synthesis, such as *gpd1* (encoding 3-phosphoglycerate dehydrogenase), is an established strategy to enhance organic acid production through the rTCA pathway in yeast (Xi et al., 2023). This strategy has been successfully applied for producing various organic acids such as lactic acid and malic acid (Zhong et al., 2021; Zhang et al., 2023). To further reduce cofactor competition, specifically NADH, in the glycerol biosynthesis pathway, we knocked out *GPD1* in strain KmSA1, generating strain KmSA2. However, *GPD1* deletion resulted in significant growth inhibition, with a maximum OD₆₀₀ of only 7.2. In addition, succinic acid titer was decreased to 6.2 g/L, but pyruvate accumulation showed no significant increase (Fig. 4f).

Collectively, these findings indicate that the knockout of *PDC1* effectively disrupted the ethanol production pathway, which significantly reduced competition for precursors and cofactors, thereby substantially enhancing the production of succinic acid. However, this strategy concurrently resulted in a notable decline in cell growth and a substantial accumulation of pyruvate. The excessive accumulation of pyruvate likely inhibited cellular metabolism and reduced the efficiency of carbon flux distribution, thereby limiting further improvements in succinic acid biosynthesis. Building on this insight, we attempted the knockout of *GPD1* to further optimize cofactor utilization and carbon flux distribution. Nevertheless, this modification severely impaired glucose metabolism,

leading to cell growth inhibition and no further increase in succinic acid production.

These findings suggest that while gene knockout strategies may significantly enhance succinic acid production, a balanced regulatory approach is essential to maintain metabolic stability and optimize carbon flux. Consequently, we selected strain KmSA1, which exhibited enhanced cell growth and increased succinic acid production, for subsequent modifications. To redirect the excess carbon flux from pyruvate towards succinic acid, we further optimized the biosynthetic pathway for producing succinic acid, thereby enhancing the efficiency of succinic acid production.

3.6. Optimizing the biosynthetic pathway of succinic acid

To enhance the catalytic efficiency of the rTCA pathway and mitigate pyruvate accumulation, we initially overexpressed the rate-limiting gene *frd*, generating strain KmSA3. Shake flask fermentation indicated that the overexpression of *frd* led to a succinic acid titer of up to 9.8 g/L. To further redirect carbon flux toward succinic acid, the copy number of *frd* was increased. However, strain KmSA4, which harbored three integrated copies of *frd*, showed no improvement in succinic acid titer, suggesting that strain KmSA3 with two copies of *frd* was the most effective strain for succinic acid production. Despite the overexpression of *frd*, pyruvate accumulation was not completely resolved.

To identify the underlying bottlenecks, we expressed and screened various *pyc*, *mdh*, and *fum* genes from multiple species in strain Km003 (Fig. 5a). Based on literature and homology analysis, we selected four *pyc* genes, three *mdh* genes, and four *fum* genes for further investigation. These heterologous genes were cloned into the episomal expression vector pURA, driven by the *PDC1* promoter, and expressed individually in strain Km003. Among the *pyc*-expressing strains, the *pyc* from *Rhizopus oryzae* exhibited the highest specific activity, showing a 130% increase compared to that of strain Km003. For the *mdh*-expressing strains, the endogenous *mdh* from *K. marxianus* displayed the highest specific activity, also reflecting a 130% enhancement over that of strain Km003. For the *fum*-expressing strains, the *fum* from *Thermus thermophilus* showed the highest specific activity, with a 190% increase over strain Km003. Consequently, we considered the integration of additional copies of pathway enzymes, *RoPYC*, *KmMDH*, and *TiFUM* into the genome of strain KmSA3 (Figs. 5b and 5c).

In strain KmSA3, we conducted individual overexpression of the genes *pyc*, *mdh*, and *fum*, as well as various combinations of these genes, constructing a series of engineered strains, KmSA5–KmSA11. Through shake flask fermentation, we evaluated which overexpression strategy achieved the most optimal balance in metabolic flux. The results revealed that strain KmSA9, which co-overexpressed *pyc* and *fum*, exhibited the highest succinic acid titer up to 13.7 g/L, reflecting a 104% increase compared to that of strain KmSA2.

To further enhance succinic acid production, we investigated the expression of succinate transporters. Previous studies have identified *SpMAE1*, a dicarboxylic acid transporter from *Schizosaccharomyces pombe*, as one of the most efficient transporters for exporting C4-dicarboxylic acids. We integrated *SpMAE1* into the NS19 locus of *K. marxianus*, generating strain KmSA12. In shake flask fermentation under oxygen-limited conditions, KmSA12 achieved a succinic acid titer of 18.7 g/L, showing a 52% increase over strain KmSA11 (Fig. 5d). These results demonstrate that facilitating the transport of intracellularly synthesized succinic acid to the extracellular space significantly enhances its accumulation. To determine whether these multiple gene integrations imposed a cellular burden, we compared protein content and metabolic activity between KmSA2 and KmSA12 (Fig. S1). KmSA12 showed an 11.5% increase in total protein content and a 6.9% reduction in metabolic activity compared to KmSA2, suggesting a measurable and manageable metabolic burden. Importantly, no significant delays in cell growth or reductions in biomass were noted during fermentation. These results indicated that while KmSA2 experienced some metabolic burden, it did not substantially compromise strain performance.

3.7 Fed-batch fermentation for succinic acid production

The engineered strain KmSA12 was subjected to fed-batch fermentation for succinic acid production. The fermentation process was initially scaled

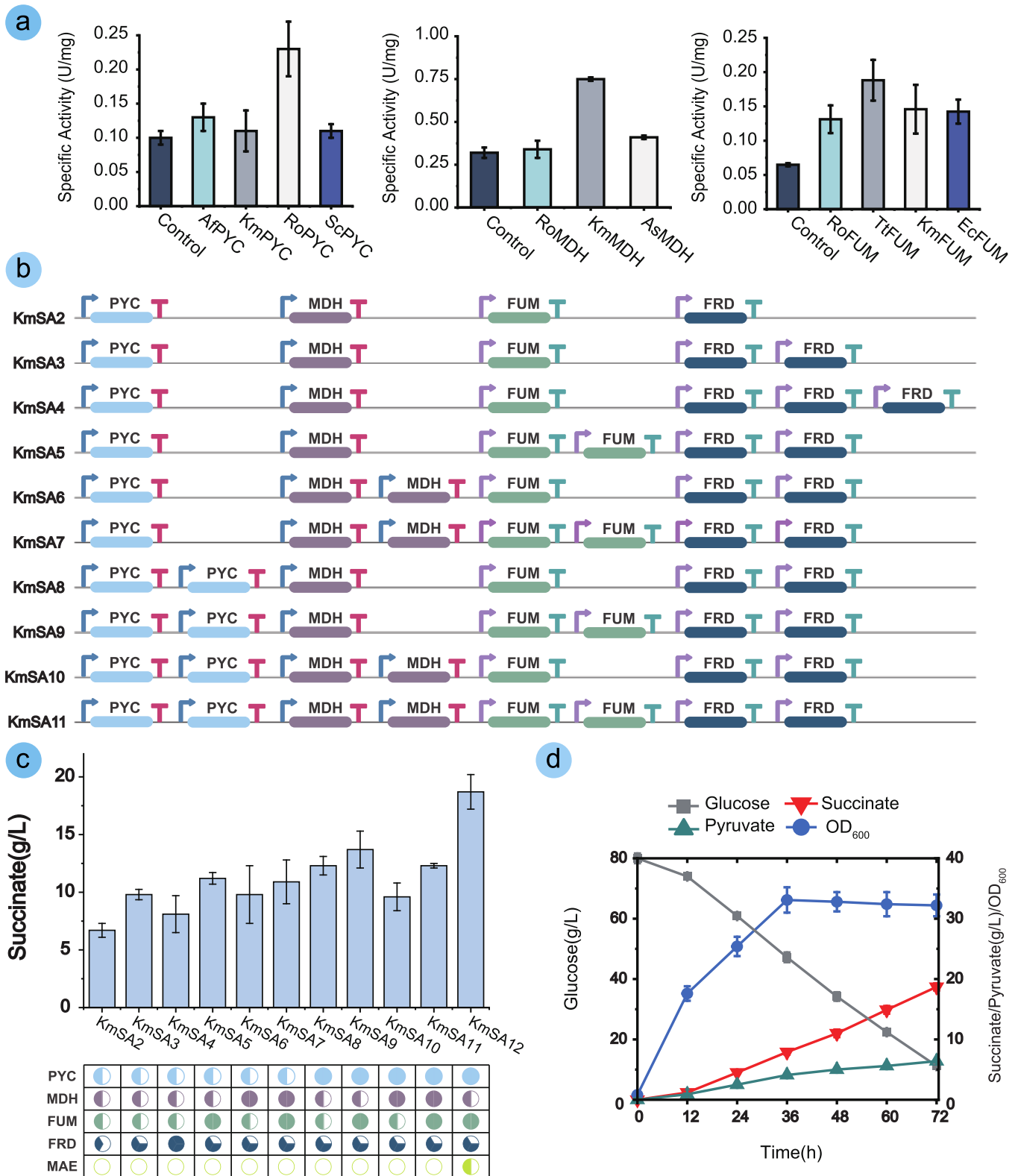


Fig. 5. Optimizing the succinic acid synthesis pathway. a: In vitro enzymatic activity analysis of pathway enzymes. Enzyme activity was quantified under optimal assay conditions. b: Increasing the copy number of pathway enzymes to balance metabolic flux. c: Effect of the copy number of pathway enzymes on the accumulation of succinic acid. d: Effect of the transporter *SpMAE1* on the accumulation of succinic acid, pyruvate, and ethanol.

up in a 5 L bioreactor at 37°C, achieving the final succinic acid titer, yield, and productivity up to 50.6 g/L, 0.31 g/g, and 0.42 g/L/h, respectively (Fig. 6a). During the initial fermentation phase, glucose was rapidly consumed and nearly depleted within 24 h. Cell growth showed an exponential phase for 36 h, and eventually reached a stable phase with minimal fluctuations. The maximum OD₆₀₀ of 53.1 was observed at 48 h. In addition, pyruvate, as the primary byproduct, demonstrated a positive correlation with succinic acid production, reaching a final titer of 7.2 g/L by the end of fermentation.

To assess the industrial potential of strain KmSA12 under thermophilic conditions, fed-batch fermentation was performed at 45°C in a 5 L bioreactor (Fig. 6b). Comparative analysis revealed a significant reduction in glucose consumption rate compared to that of fermentation at 37°C. With progressive glucose consumption, succinic acid was gradually accumulated, indicating that the metabolic functionality of strain KmSA12 was maintained despite the elevated temperature. By 120 h, the total glucose consumption reached 151.6 g/L, representing a 7.4% reduction compared to

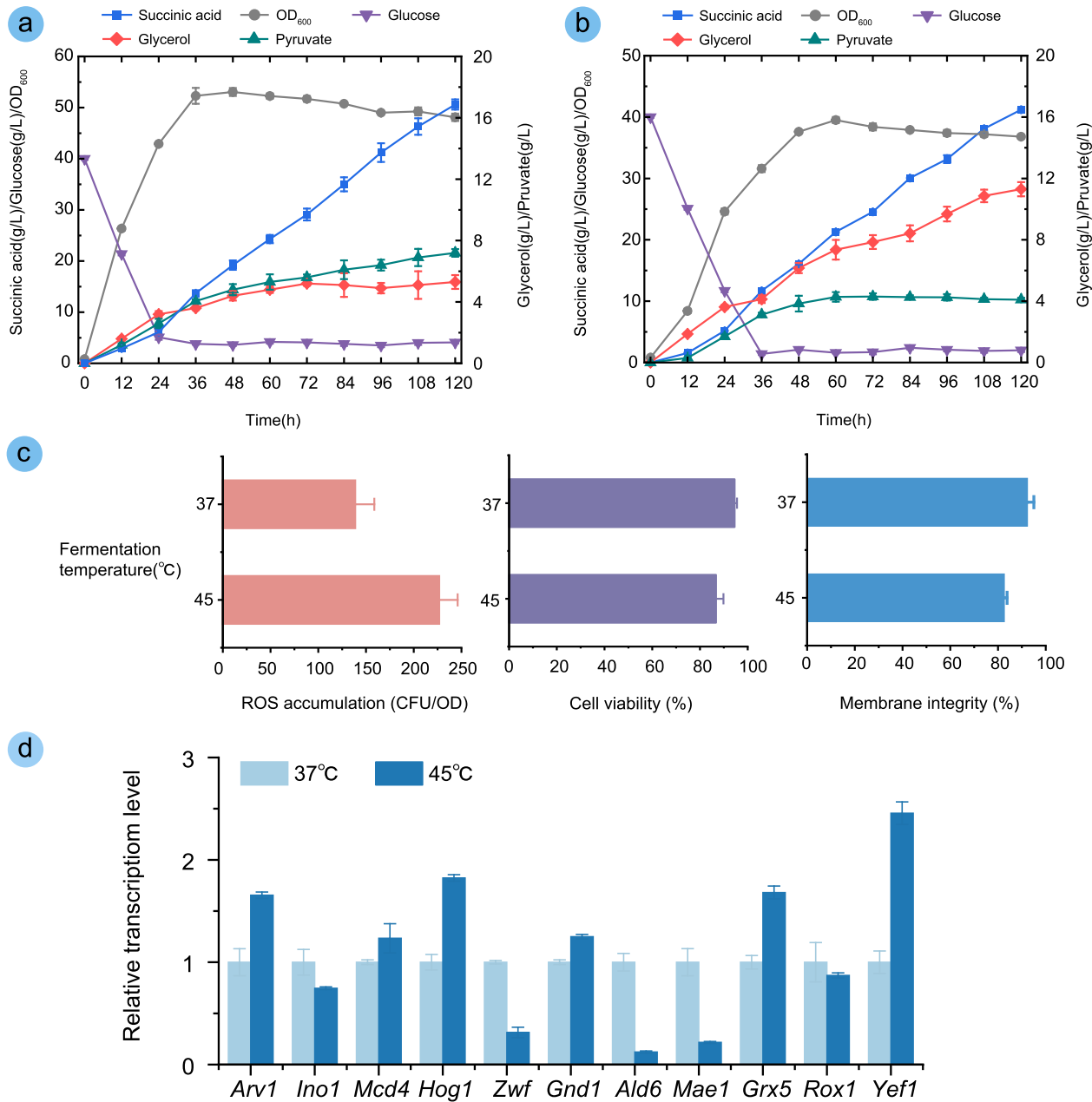


Fig. 6. Fed-batch fermentation for succinic acid production. **a:** Fed-batch fermentation with strain KmSA12 at 37°C. **b:** Fed-batch fermentation with strain KmSA12 at 45°C. **c:** Comparison of ROS accumulation, cell survival rate, and membrane integrity between different fermentation conditions. **d:** qPCR validation of the stress-related and redox-associated genes under different fermentation conditions. ARV1: a membrane protein implicated in lipid homeostasis and sterol transport; INO1: myo-inositol-1-phosphate synthase, crucial for phospholipid biosynthesis; MCD4: an acyltransferase involved in the biosynthesis of glycosylphosphatidylinositol anchors, which are vital for maintaining cell wall integrity; HOG1: a mitogen-activated protein kinase integral to the high-osmolarity glycerol (HOG) signaling pathway, which is also activated by heat and oxidative stress; GRX5: a mitochondrial glutaredoxin that plays a role in iron-sulfur cluster assembly and oxidative defense; ROX1: heme-dependent transcriptional repressor of hypoxic genes; ZWF1: glucose-6-phosphate dehydrogenase, the initiator of the oxidative pentose phosphate pathway; GND1 6-phosphogluconate dehydrogenase, which further contributes to NADPH synthesis; ALD6 NADP⁺-dependent aldehyde dehydrogenase; MAE1: mitochondrial malic enzyme; YEF1: ATP-binding cassette transporter.

that of fermentation at 37°C. Cellular growth achieved a maximum OD₆₀₀ of 39.5 at 60 h, which was 18.7% lower than that of fermentation at 37°C. Additionally, glycerol accumulation exhibited a temperature-dependent increase, reaching a titer of 11.3 g/L, which was 113.2% higher than that of fermentation at 37°C. Following 120 h fermentation, the final titer, yield, and productivity of succinic acid reached 41.2 g/L, 0.27 g/g, and 0.34 g/L/h, respectively. The final pH reached 3.42, which remained within the acid tolerance range of strain KmSA12 (Fig. S2). The titer, yield, and productivity of succinic acid represented an 18.6%, 12.9% and 19.0% decrease compared to that of fermentation at 37°C, respectively. However, the productivity remained stable at 0.30 g/L/h during the latter phase of fermentation (96–120 h), indicating that strain KmSA12 retained significant metabolic capacity for succinic acid production under thermophilic conditions. These results indicated that strain KmSA12 had notable thermal tolerance and industrial potential for succinic acid production at high temperatures.

To further explore the physiological mechanisms behind strain robustness against thermal and acid stress, we assessed intracellular ROS accumulation, cell viability, and membrane integrity during fermentation at 45°C (Fig. 6c). When compared to fermentation at 37°C, fermentation at 45°C led to a significant increase in intracellular ROS levels. At the same time, cell viability and membrane integrity were decreased by 8.3% and 10.6%, respectively. These findings suggested that high temperatures (45°C) resulted in oxidative stress and damage to membrane structure, but the engineered *K. marxianus* KmSA12 still exhibited relatively high viability and membrane integrity, indicating its thermotolerance. Additionally, qRT-PCR analysis was conducted on genes associated with acid stress (ARV1, INO1, MCD4), oxidative stress (HOG1, GRX5, ROX1), and NADPH regeneration or transport (ZWF, GND1, ALD6, Mae1, YEF1) (Fig. 6d). Under low-pH and high-temperature conditions, ARV1, MCD4, HOG1, GND1, GRX5, and YEF1 were upregulated, while INO1, ZWF, ALD6, and Mae1 were downregulated. These results indicate that the engineered strain activates protective and redox-balancing mechanisms in response to acid accumulation and heightened metabolic flux.

Traditional fermentation at 30 to 37°C often requires chilled water or refrigeration to maintain temperature, especially in large-scale operations. In contrast, fermentation at 45°C is aligned with ambient temperatures in many regions, negating the need for refrigeration. This change reduces energy consumption for cooling, cuts utility costs, and enhances sustainability. Furthermore, 45°C falls within the optimal range for various lignocellulose-degrading enzymes, enabling direct integration of fermentation with upstream saccharification processes and eliminating pre-fermentation cooling requirements (Wu et al., 2021). Additionally, high-temperature fermentation naturally deters microbial contamination, as common contaminants like lactic acid bacteria and wild-type yeasts show limited growth above 42°C (Chen et al., 2023).

Traditional bacterial fermentations usually require significant neutralization, such as MgCO₃ and CaCO₃, followed by post-fermentation acidification with H₂SO₄ to acidify succinate or adjust pH for extraction. The highest reported succinic acid recovery to date is 79% through acidification followed by direct crystallization (Oreoluwa Jokodola et al., 2022). These pH modification steps contribute to nearly 50% of the total cost (Alexandri et al., 2019). Conversely, the minimal neutralization strategy in *K. marxianus* KmSA12 fermentation simplifies purification. With a final broth pH of 3.42, downstream recovery processes such as direct crystallization, liquid-liquid extraction, or electrodialysis can proceed with little to no post-fermentation acidification. This approach reduces salt accumulation, thereby enhancing product purity and lessening the environmental impact of salt-laden wastewater. This work marks a significant advancement in developing *K. marxianus* as a platform for bio-based chemical production, highlighting its substantial potential for industrial-scale applications.

The physiological mechanisms underlying strain robustness against acid stress require further investigation. Currently, several mechanisms have been reported to be involved in acid-tolerance regulation, such as proton pump activity, ATP-binding cassette (ABC) transporters, intracellular pH homeostasis, glycosylphosphatidylinositol (GPI)-anchored protein-related cell wall remodeling, and plasma membrane ergosterol levels (Lv et al., 2023). Notably, *S. cerevisiae* adapts to acetic acid stress through the regulation of ergosterol biosynthesis and cell wall rigidity. The Pdr18

transporter is crucial in this adaptation through promoting ergosterol incorporation into membranes to maintain structural integrity and enabling dynamic cell wall restructuring (Ribeiro et al., 2022). This dual mechanism effectively reduces membrane permeability and enhances mechanical strength during acid exposure.

Microbial tolerance to ionic liquids has also been highlighted, which are prevalent inhibitors found in lignocellulosic hydrolysates (Lugani et al., 2020). Significant advances have been made in engineering strains with increased ionic liquid resistance through membrane composition modifications and specialized transporter expression (Cheah et al., 2020). These developments are crucial for biorefineries, where inhibitor tolerance affects bioconversion efficiency. For *K. marxianus* KmSA12, these advances suggest promising strategies for strain enhancement: engineering the cell membrane to improve stability under low pH and solvent stress, optimizing stress response pathways to sustain redox and osmotic homeostasis, and improving transport mechanisms to bolster resilience against ionic liquids and other inhibitors. These approaches could significantly improve the robustness of KmSA12 in industrial-scale succinic acid production, thereby contributing to a sustainable and efficient process.

4. Conclusions

In this study, *K. marxianus* was metabolically engineered as a robust platform for succinic acid biosynthesis. As an unconventional yeast, *K. marxianus* is intrinsically resistant to high temperatures and acidic conditions, along with rapid growth characteristics. We first developed a series of novel genetic manipulation tools tailored specifically for *K. marxianus*, including a CRISPR-Cas9 gene editing system, an endogenous promoter library for precise gene expression, and a neutral integration site library. These tools significantly improved the precision and efficiency of genetic modifications. Subsequently, we constructed and optimized the biosynthetic pathway of succinic acid by analyzing pathway byproducts, balancing metabolic flux, and enhancing the succinic acid transport system. Finally, fed-batch fermentation of strain KmSA12 in a 50 L bioreactor achieved succinic acid titer, yield, and productivity up to 50.6 g/L, 0.31 g/g, and 0.42 g/L/h, respectively. These advancements establish a promising non-conventional yeast platform for succinic acid production, providing a foundation for developing a benchmark for bio-based production of organic acids.

Acknowledgements

This work was financially supported by the National Natural Science Foundation of China (22378166), the Basic Research Program of Jiangsu and Jiangsu Basic Research Center for Synthetic Biology (BK20233003), the Fundamental Research Funds for the Central Universities (JUSRP622001), and the Open Funding Project of Key Laboratory of Industrial Biotechnology Ministry of Education (KLIB-KF202403).

Author contribution

Ziyun Gu: Methodology, Investigation, Formal analysis, Data curation, Resources, Supervision, Visualization, Writing - original draft. **Deyang Ding:** Methodology, Formal analysis, Data curation, Resources, Supervision, Writing - review & editing. **Zhanpeng Shan:** Methodology, Formal analysis, Supervision, Writing - review & editing. **Yongsheng Tang:** Formal analysis, Validation, Supervision, Writing - review & editing. **Xiulai Chen:** Conceptualization, Methodology, Validation, Resources, Supervision, Project administration, Funding acquisition, Writing - review & editing.

Conflict of interest

The authors declare that they have no conflicts of interest to disclose.

References

- [1] Ahn, J.H., Jang, Y.S., Lee, S.Y., 2016. Production of succinic acid by metabolically engineered microorganisms. *Curr. Opin. Biotechnol.* 42, 54-66.

- [2] Alexandri, M., Vlysidis, A., Papapostolou, H., Tverezovskaya, O., Tverezovskiy, V., Kookos, I.K., Koutinas, A., 2019. Downstream separation and purification of succinic acid from fermentation broths using spent sulphite liquor as feedstock. *Sep. Purif. Technol.* 209, 666-675.
- [3] Antunes, D.F., de Souza Junior, C.G., de Morais Junior, M.A., 2000. A simple and rapid method for lithium acetate-mediated transformation of *Kluyveromyces marxianus* cells. *World J. Microbiol. Biotechnol.* 16(7), 653-654.
- [4] Bozell, J.J., Petersen, G.R., 2010. Technology development for the production of biobased products from biorefinery carbohydrates—the US department of energy’s “top 10” revisited. *Green Chem.* 12(4), 539-554.
- [5] Bradford, M.M., 1976. A rapid and sensitive method for the quantitation of microgram quantities of protein utilizing the principle of protein-dye binding. *Anal. Biochem.* 72(1), 248-254.
- [6] Cheah, W.Y., Sankaran, R., Pau, L.S., Ibrahim, T., Chew, K.W., Culaba, A., Chang, J.S., 2020. Pretreatment methods for lignocellulosic biofuels production: current advances, challenges and future prospects. *Biofuel Res. J.* 7(1), 1115-1127.
- [7] Chen, Z., Liu, J., Han, X., Ma, L., Xu, P., Tao, F., 2023. Developing a thermophilic cell factory for high-temperature production of 1,3-propanediol via host-mining and metabolic engineering. *Chem Catal.* 3(8), 100704.
- [8] Choi, S., Song, C.W., Shin, J.H., Lee, S.Y., 2015. Biorefineries for the production of top building block chemicals and their derivatives. *Metab. Eng.* 28, 223-239.
- [9] Chung, S.C., Park, J.S., Yun, J., Park, J.H., 2017. Improvement of succinate production by release of end-product inhibition in *Corynebacterium glutamicum*. *Metab. Eng.* 40, 157-164.
- [10] Cok, B., Tsiropoulos, I., Roes, A.L., Patel, M.K., 2014. Succinic acid production derived from carbohydrates: an energy and greenhouse gas assessment of a platform chemical toward a bio-based economy. *Biofuels Bioprod. Biorefin.* 8(1), 16-29.
- [11] Cui, Z., Zhong, Y., Sun, Z., Jiang, Z., Deng, J., Wang, Q., Nielsen, J., Hou, J., Qi, Q., 2023. Reconfiguration of the reductive TCA cycle enables high-level succinic acid production by *Yarrowia lipolytica*. *Nat. Commun.* 14(1), 8480.
- [12] Dunayevich, P., Baltanás, R., Clemente, J.A., Couto, A., Sapochnik, D., Vasen, G., Colman-Lerner, A., 2018. Heat-stress triggers MAPK crosstalk to turn on the hyperosmotic response pathway. *Sci. Rep.* 8(1), 15168.
- [13] Eszterhas, S.K., E., B.E., K., M.D.I., and Fiering, S., 2002. Transcriptional interference by independently regulated genes occurs in any relative arrangement of the genes and is influenced by chromosomal integration position. *Mol. Cell. Biol.* 22(2), 469-479.
- [14] Geng, K., Lin, Y., Zheng, X., Li, C., Chen, S., Ling, H., Yang, J., Zhu, X., Liang, S., 2024. Enhanced expression of alcohol dehydrogenase i in *Pichia pastoris* reduces the content of acetaldehyde in wines. *Microorganisms.* 12(1), 38.
- [15] Jansen, M.L.A., van Gulik, W.M., 2014. Towards large scale fermentative production of succinic acid. *Curr. Opin. Biotechnol.* 30, 190-197.
- [16] Jiang, M., Ma, J., Wu, M., Liu, R., Liang, L., Xin, F., Zhang, W., Jia, H., Dong, W., 2017. Progress of succinic acid production from renewable resources: metabolic and fermentative strategies. *Bioresour. Technol.* 245, 1710-1717.
- [17] Kumar, R., Basak, B., Jeon, B.H., 2020. Sustainable production and purification of succinic acid: a review of membrane-integrated green approach. *J. Clean. Prod.* 277, 123954.
- [18] Lee, J.A., Ahn, J.H., Lee, S.Y., 2019. Organic acids: succinic and malic acids, *Compr Biotechnol.* Elsevier, pp. 172-187.
- [19] Lee, J.W., Yi, J., Kim, T.Y., Choi, S., Ahn, J.H., Song, H., Lee, M.-H., Lee, S.Y., 2016. Homo-succinic acid production by metabolically engineered *Mannheimia succiniciproducens*. *Metab. Eng.* 38, 409-417.
- [20] Lertwattanasakul, N., Kosaka, T., Hosoyama, A., Suzuki, Y., Rodrussamee, N., Matsutani, M., Murata, M., Fujimoto, N., Suprayogi, Tsuchikane, K., Limtong, S., Fujita, N., Yamada, M., 2015. Genetic basis of the highly efficient yeast *Kluyveromyces marxianus*: complete genome sequence and transcriptome analyses. *Biotechnol. Biofuels.* 8(1), 47.
- [21] Li, K., Li, C., Zhao, X.Q., Liu, C.G., Bai, F.W., 2023. Engineering *Corynebacterium glutamicum* for efficient production of succinic acid from corn stover pretreated by concentrated-alkali under steam-assistant conditions. *Bioresour. Technol.* 378, 128991.
- [22] Liu, X., Zhao, G., Sun, S., Fan, C., Feng, X., Xiong, P., 2022a. Biosynthetic pathway and metabolic engineering of succinic acid. *Front. Bioeng. Biotechnol.* 10, 843887.
- [23] Liu, Z.W., Simmons, C.H., Zhong, X., 2022b. Linking transcriptional silencing with chromatin remodeling, folding, and positioning in the nucleus. *Curr. Opin. Plant. Biol.* 69, 102261.
- [24] Lugani, Y., Rai, R., Prabhu, A.A., Maan, P., Hans, M., Kumar, V., Kumar, S., Chandel, A.K., Sengar, R.S., 2020. Recent advances in bioethanol production from lignocelluloses: a comprehensive review with a focus on enzyme engineering and designer biocatalysts. *Biofuel Res. J.* 7(4), 1267-1295.
- [25] Lv, X., Jin, K., Yi, Y., Song, L., Xiu, X., Liu, Y., Li, J., Du, G., Chen, J., Liu, L., 2023. Analysis of acid-tolerance mechanism based on membrane microdomains in *Saccharomyces cerevisiae*. *Microb. Cell. Fact.* 22(1), 180.
- [26] Oreoluwa Jokodola, E., Narisetty, V., Castro, E., Durgapal, S., Coulon, F., Sindhu, R., Binod, P., Rajesh Banu, J., Kumar, G., Kumar, V., 2022. Process optimisation for production and recovery of succinic acid using xylose-rich hydrolysates by *Actinobacillus succinogenes*. *Bioresour. Technol.* 344(Part B), 126224.
- [27] Pan, J., Tang, Y., Liu, J., Gao, C., Song, W., Wu, J., Liu, L., Chen, X., 2024. Reprogramming protein stability in *Escherichia coli* to improve four-carbon dicarboxylic acids production. *Chem. Eng. J.* 493, 152893.
- [28] Rajkumar, A.S., Varela, J.A., Juergens, H., Daran, J.M.G., Morrissey, J.P., 2019. Biological parts for *Kluyveromyces marxianus* synthetic biology. *Front. Bioeng. Biotechnol.* 7, 97.
- [29] Rendulić, T., Perpelea, A., Ortiz, J.P.R., Casal, M., Nevoigt, E., 2024. Mitochondrial membrane transporters as attractive targets for the fermentative production of succinic acid from glycerol in *Saccharomyces cerevisiae*. *FEMS yeast Res.* 24, foae009.
- [30] Ribeiro, R.A., Godinho, C.P., Vitorino, M.V., Robalo, T.T., Fernandes, F., Rodrigues, M.S., Sá-Correia, I.J.J.o.F., 2022. Crosstalk between yeast cell plasma membrane ergosterol content and cell wall stiffness under acetic acid stress involving Pdr18. *J. Fungi.* 8(2), 103.
- [31] Riles, L., Fay, J.C., 2019. Genetic basis of variation in heat and ethanol tolerance in *Saccharomyces cerevisiae*. *G3.* 9(1), 179-188.
- [32] Takayama, Y., Takahashi, K., 2007. Differential regulation of repeated histone genes during the fission yeast cell cycle. *Nucleic Acids Res.* 35(10), 3223-3237.
- [33] Tran, V.G., Mishra, S., Bhagwat, S.S., Shafaei, S., Shen, Y., Allen, J.L., Crosly, B.A., Tan, S.-I., Fatma, Z., Rabinowitz, J.D., Guest, J.S., Singh, V., Zhao, H., 2023. An end-to-end pipeline for succinic acid production at an industrially relevant scale using *Issatchenkia orientalis*. *Nat. Commun.* 14(1), 6152.
- [34] Wang, X., Pan, J., Wu, J., Chen, X., Gao, C., Song, W., Wei, W., Liu, J., Liu, L., 2023. Regulation of intracellular level of ATP and NADH in *Escherichia coli* to promote succinic acid production. *Chin. J. Biotechnol.* 39(8), 3236-3252.
- [35] Werpy, T., Petersen, G., Aden, A., Bozell, J., Holladay, J.J.S.F., 2004. Top value added chemicals from biomass: I. Results of screening for potential candidates from sugars and synthesis gas. *Office of Scientific and Technical Information* 69, 1-65.
- [36] Wu, Y., Wang, Z., Ma, X., Xue, C., 2021. High temperature simultaneous saccharification and fermentation of corn stover for efficient butanol production by a thermotolerant *Clostridium acetobutylicum*. *Process Biochem.* 100, 20-25.
- [37] Xi, Y., Xu, H., Zhan, T., Qin, Y., Fan, F., Zhang, X., 2023. Metabolic engineering of the acid-tolerant yeast *Pichia kudriavzevii* for efficient L-malic acid production at low pH. *Metab. Eng.* 75, 170-180.
- [38] Xiong, L., Zeng, Y., Tang, R.Q., Alper, H.S., Bai, F.W., Zhao, X.Q., 2018. Condition-specific promoter activities in *Saccharomyces cerevisiae*. *Microb. Cell. Fact.* 17(1), 58.

- [39] Yadav, V.G., De Mey, M., Giaw Lim, C., Kumaran Ajikumar, P., Stephanopoulos, G., 2012. The future of metabolic engineering and synthetic biology: towards a systematic practice. *Metab. Eng.* 14(3), 233-241.
- [40] Yang, Q., Wu, M., Dai, Z., Xin, F., Zhou, J., Dong, W., Ma, J., Jiang, M., Zhang, W., 2020. Comprehensive investigation of succinic acid production by *Actinobacillus succinogenes*: a promising native succinic acid producer. *Biofuels Bioprod. Biorefin.* 14(5), 950-964.
- [41] Zhang, B., Li, R., Yu, L., Wu, C., Liu, Z., Bai, F., Yu, B., Wang, L., 2023. l-Lactic Acid Production via Sustainable Neutralizer-Free Route by Engineering Acid-Tolerant Yeast *Pichia kudriavzevii*. *J. Agric. Food Chem.* 71(29), 11131-11140.
- [42] Zhong, W., Yang, M., Hao, X., Sharshar, M.M., Wang, Q., Xing, J., 2021. Improvement of D-lactic acid productivity by introducing *Escherichia coli* acetyl-CoA synthesis pathway in engineered *Saccharomyces cerevisiae*. *J. Chem. Technol. Biotechnol.* 96(9), 2509-2519.
- [43] Zhong, Y., Shang, C., Wang, Y., Li, J., Liu, C., Cui, Z., Qi, Q., 2024. Advances in synthesis of succinic acid using yeast cell factories. *Chin. J. Biotechnol.* 40(8), 2644-2665.
- [44] Zhou, H., Tian, T., Liu, J., Lu, H., Yu, Y., Wang, Y., 2024. Efficient and markerless gene integration with SlugCas9-HF in *Kluyveromyces marxianus*. *Commun. Biol.* 7(1), 797.
- [45] Zhu, X., Tan, Z., Xu, H., Chen, J., Tang, J., Zhang, X., 2014. Metabolic evolution of two reducing equivalent-conserving pathways for high-yield succinate production in *Escherichia coli*. *Metab. Eng.* 24, 87-96.



Ziyun Gu is a postgraduate student in the School of Biotechnology at Jiangnan University. His research focuses on metabolic engineering of yeasts for organic acids biosynthesis.



Yongsheng Tang is a postgraduate student in the School of Biotechnology at Jiangnan University. His research focuses on metabolic engineering of bacteria for organic acids biosynthesis.



Deyang Ding is a postgraduate student in the School of Biotechnology at Jiangnan University. His research focuses on metabolic engineering of yeasts for organic acids biosynthesis.



Zhanpeng Shan is a postgraduate student in the School of Biotechnology at Jiangnan University. His research focuses on metabolic engineering of yeasts for the biosynthesis of natural products.



Prof. Xiulai Chen is a Professor at Jiangnan University. He received his Ph.D. degree in Fermentation Engineering from Jiangnan University in 2015. Following his Ph.D., he worked at the University of California at Berkeley as a postdoctoral fellow, focusing on the biosynthesis of natural products in 2019. Currently, his research focuses on microbial metabolic engineering and synthetic biology. He has published more than 140 international peer-reviewed journal papers, including *Nature*, *Nature Catalysis*, *Nature Communications*, *Energy & Environmental Science*, *Chem*, *Angewandte Chemie International Edition*, *Chemical Reviews*.

Supplementary Information

Table S1.

Strains used in this study.

Strain	Description	Source
<i>E. coli</i> JM109	General cloning host	This Lab
<i>K. marxianus</i> NBRC1777	<i>K. marxianus</i> Wild type	
<i>K. marxianus</i> Km001	<i>K. marxianus</i> NBRC1777 Δ ura3	This Study
<i>K. marxianus</i> Km002	<i>K. marxianus</i> NBRC1777 Δ ura3 Δ leu2	
<i>K. marxianus</i> Km003	<i>K. marxianus</i> NBRC1777 Δ ura3 Δ leu2 Δ trp1	
<i>K. marxianus</i> Km004	<i>K. marxianus</i> NBRC1777 Δ ura3 Δ leu2 Δ trp1 Δ ade1	
<i>K. marxianus</i> SA	<i>K. marxianus</i> Km003- <i>Afpyc-Asmdh-Ecfum-Tbfrd</i>	
<i>K. marxianus</i> SA1	<i>K. marxianus</i> SA <i>Apdc1</i>	
<i>K. marxianus</i> SA2	<i>K. marxianus</i> SA <i>Agpd1</i>	
<i>K. marxianus</i> SA3	<i>K. marxianus</i> SA2- <i>Tbfrd</i>	
<i>K. marxianus</i> SA4	<i>K. marxianus</i> SA3- <i>Tbfrd</i>	
<i>K. marxianus</i> SA5	<i>K. marxianus</i> SA3- <i>Tfjum</i>	
<i>K. marxianus</i> SA6	<i>K. marxianus</i> SA3- <i>Knmndh</i>	
<i>K. marxianus</i> SA7	<i>K. marxianus</i> SA3- <i>Knmndh-Tifum</i>	
<i>K. marxianus</i> SA8	<i>K. marxianus</i> SA3- <i>Ropyc</i>	
<i>K. marxianus</i> SA9	<i>K. marxianus</i> SA3- <i>Ropyc-Tfjum</i>	
<i>K. marxianus</i> SA10	<i>K. marxianus</i> SA3- <i>Ropyc-Knmndh</i>	
<i>K. marxianus</i> SA11	<i>K. marxianus</i> SA3- <i>Ropyc-Knmndh-Tifum</i>	
<i>K. marxianus</i> SA12	<i>K. marxianus</i> SA11- <i>Spmae1</i>	

Table S2.

Plasmids used in this study.

Plasmid	Description
pURA	<i>panars</i> , <i>amp</i> , <i>ura3</i> , P _{PDC1}
pCAS9	<i>panars</i> , <i>amp</i> , <i>ura3</i> , P _{TEF-cas9} , P _{GPD-N20}
pCAS9-ADE1	<i>panars</i> , <i>amp</i> , <i>ura3</i> , P _{TEF-cas9} , P _{GPD-N20} (<i>ade1</i> :TGC GTTCGGCAATGTCTTGA)
pCAS9-PDC1	<i>panars</i> , <i>amp</i> , <i>ura3</i> , P _{TEF-cas9} , P _{GPD-N20} (<i>pdcl</i> :ACGAAGTCCCAGGTATGAGA)
pCAS9-GPD1	<i>panars</i> , <i>amp</i> , <i>ura3</i> , P _{TEF-cas9} , P _{GPD-N20} (<i>gpd1</i> :TCCTCATCAATTTTTGCCAA)
pCUT1	<i>panars</i> , <i>amp</i> , <i>ura3</i> , P _{TEF-cas9} , P _{GPD-N20} (NS1:TCTCGGCTTAGAGATCTGTG)
pCUT1	<i>panars</i> , <i>amp</i> , <i>ura3</i> , P _{TEF-cas9} , P _{GPD-N20} (NS2:AGGATGTTCCGATATAGACGA)
pCUT3	<i>panars</i> , <i>amp</i> , <i>ura3</i> , P _{TEF-cas9} , P _{GPD-N20} (NS3:ACGTTTGCAGAGGATCTGCG)
pCUT4	<i>panars</i> , <i>amp</i> , <i>ura3</i> , P _{TEF-cas9} , P _{GPD-N20} (NS4:CCAGAACTTTATATCCTGGG)
pCUT5	<i>panars</i> , <i>amp</i> , <i>ura3</i> , P _{TEF-cas9} , P _{GPD-N20} (NS5:ATACGTAACGTCCCACCCAG)
pCUT6	<i>panars</i> , <i>amp</i> , <i>ura3</i> , P _{TEF-cas9} , P _{GPD-N20} (NS6:AGTGCCCTAAAGTGACCGGG)
pCUT1	<i>panars</i> , <i>amp</i> , <i>ura3</i> , P _{TEF-cas9} , P _{GPD-N20} (NS7:CAACGCTAGCATTTACGGG)
pCUT8	<i>panars</i> , <i>amp</i> , <i>ura3</i> , P _{TEF-cas9} , P _{GPD-N20} (NS8:GAGCGCCAATGTATGAACGG)
pCUT9	<i>panars</i> , <i>amp</i> , <i>ura3</i> , P _{TEF-cas9} , P _{GPD-N20} (NS9:AAGCGGTTATTACATAGTGG)
pCUT10	<i>panars</i> , <i>amp</i> , <i>ura3</i> , P _{TEF-cas9} , P _{GPD-N20} (NS10:TTAGTGACGGTAACACACCG)
pCUT11	<i>panars</i> , <i>amp</i> , <i>ura3</i> , P _{TEF-cas9} , P _{GPD-N20} (NS11:ACCCTGCTCTACAATCTACG)
pCUT12	<i>panars</i> , <i>amp</i> , <i>ura3</i> , P _{TEF-cas9} , P _{GPD-N20} (NS12:GGGATTCAGAAATATCCGGA)
pCUT13	<i>panars</i> , <i>amp</i> , <i>ura3</i> , P _{TEF-cas9} , P _{GPD-N20} (NS13:GCGGAATGGCATTCACTACG)

Table S2.
continued.

Plasmid	Description
pCUT14	<i>panars, amp, ura3, P_{TEF}-cas9, P_{GPD}-N20 (NS14:GTAACGTAACCGTAGTACCG)</i>
pCUT15	<i>panars, amp, ura3, P_{TEF}-cas9, P_{GPD}-N20 (NS15:TATCGCTGTTCAATGTACCG)</i>
pCUT16	<i>panars, amp, ura3, P_{TEF}-cas9, P_{GPD}-N20 (NS16:GTTGTAATAGACGCGCTATG)</i>
pCUT17	<i>panars, amp, ura3, P_{TEF}-cas9, P_{GPD}-N20 (NS17:AAGTAGTTACTAACGCACGG)</i>
pCUT18	<i>panars, amp, ura3, P_{TEF}-cas9, P_{GPD}-N20 (NS18:GACCGAGCAAGCAACTACAG)</i>
pCUT19	<i>panars, amp, ura3, P_{TEF}-cas9, P_{GPD}-N20 (NS19:ATGGGCATAAGAAAGGTATG)</i>
pCUT20	<i>panars, amp, ura3, P_{TEF}-cas9, P_{GPD}-N20 (NS20:GACACGGAGCGCAAACACGT)</i>
pGFP	<i>Ars7/cen, amp, leu2, P_{ScTEF}-egfp</i>
pGFP-TEF1	<i>Ars7/cen, amp, leu2, P_{TEF1}-egfp</i>
pGFP-PDC1	<i>Ars7/cen, amp, leu2, P_{PDC1}-egfp</i>
pGFP-PGK1	<i>Ars7/cen, amp, leu2, P_{PGK1}-egfp</i>
pGFP-GPD1	<i>Ars7/cen, amp, leu2, P_{GPD1}-egfp</i>
pGFP-TEF4	<i>Ars7/cen, amp, leu2, P_{TEF4}-egfp</i>
pGFP-FBA1	<i>Ars7/cen, amp, leu2, P_{FBA1}-egfp</i>
pGFP-HHF1	<i>Ars7/cen, amp, leu2, P_{HHF1}-egfp</i>
pGFP-HHF2	<i>Ars7/cen, amp, leu2, P_{HHF2}-egfp</i>
pGFP-GPD2	<i>Ars7/cen, amp, leu2, P_{GPD2}-egfp</i>
pGFP-ENO1	<i>Ars7/cen, amp, leu2, P_{ENO1}-egfp</i>
pGFP-GDH2	<i>Ars7/cen, amp, leu2, P_{GDH2}-egfp</i>
pGFP-REV1	<i>Ars7/cen, amp, leu2, P_{REV1}-egfp</i>
pGFP-HSP26	<i>Ars7/cen, amp, leu2, P_{HSP26}-egfp</i>
pGFP-MDH1	<i>Ars7/cen, amp, leu2, P_{MDH1}-egfp</i>
pGFP-MDH2	<i>Ars7/cen, amp, leu2, P_{MDH2}-egfp</i>
pGFP-CIT1	<i>Ars7/cen, amp, leu2, P_{CIT1}-egfp</i>
pGFP-ADH1	<i>Ars7/cen, amp, leu2, P_{ADH1}-egfp</i>
pGFP-ADH2	<i>Ars7/cen, amp, leu2, P_{ADH2}-egfp</i>
pGFP-XYL1	<i>Ars7/cen, amp, leu2, P_{XYL1}-egfp</i>
pGFP-HHT1	<i>Ars7/cen, amp, leu2, P_{HHT1}-egfp</i>

Table S4.
Neutral sites used in this study.

Site	N20	Chromosome	Location
neutral sites 1	TCTCGGCTTAGAGATCTGTG	1	65590
neutral sites 2	AGGATGTTTCGATATAGACGA	1	1349684
neutral sites 3	ACGTTTGCAGAGGATCTGCG	1	119880
neutral sites 4	CCAGAACTTTATATCTCGGG	2	116211
neutral sites 5	ATACGTAACGTCCCACCCAG	2	1429650
neutral sites 6	AGTGCCCTAAAGTGACCGGG	2	1045039
neutral sites 7	CAACGTCTAGCATTACGGG	2	1225053
neutral sites 8	GAGCGCCAATGTATGAACGG	3	1054394
neutral sites 9	AAGCGTTATTACATAGTGG	3	1206444
neutral sites 10	TTAGTGACGGTAACACACCG	3	797969
neutral sites 11	ACCCTGCTCTACAATCTACG	4	488419
neutral sites 12	GGGATTCAGAAATATCCGGA	4	253799
neutral sites 13	GCGGAATGCGATTCACTACG	4	934729
neutral sites 14	GTAACGTAACCGTAGTACCG	5	791444
neutral sites 15	TATCGCTGTCAATGTACCG	6	1018789
neutral sites 16	GTTGTAATAGACGCGCTATG	6	703537
neutral sites 17	AAGTAGTTACTAACGCACGG	7	741626
neutral sites 18	GACCGAGCAAGCAACTACAG	7	538009
neutral sites 19	ATGGGCATAAGAAAGGTATG	8	316445
neutral sites 20	GACACGGAGCGCAAACACGT	8	31637

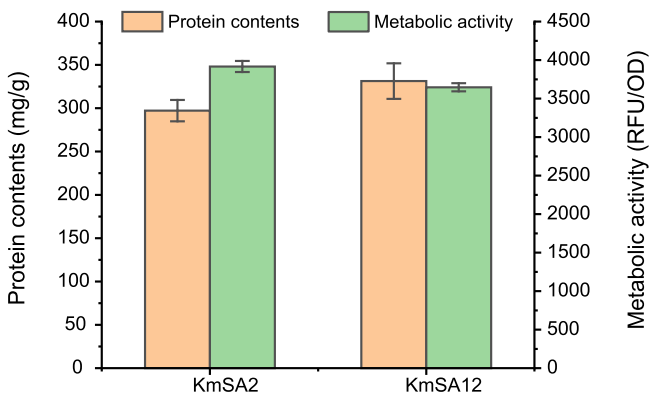


Fig. S1. Comparison of metabolic activity and protein stability between KmSA2 and KmSA12.

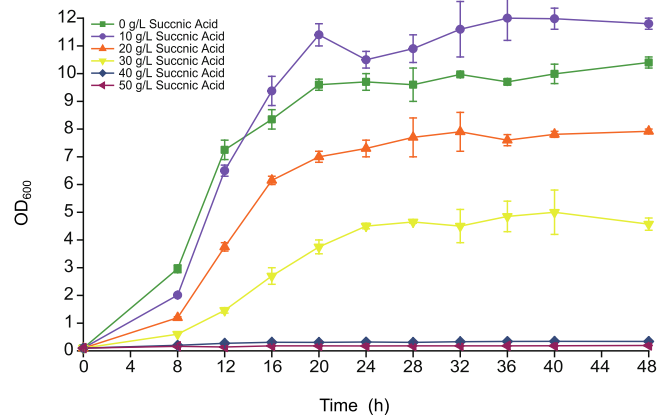


Fig. S2. Cell growth of KmSA12 under different succinic acid concentrations.